

Effect of Coulomb screening on the discrete scale invariance of quasibound states in three-dimensional topological semimetals

Hongchao Liu¹, Haiwen Liu^{2,*}, Robert Joynt^{3,4} and X. C. Xie^{1,5}

¹*International Center for Quantum Materials, Peking University, Beijing 100871, China*

²*Center for Advanced Quantum Studies, Department of Physics, Beijing Normal University, Beijing 100875, China*

³*Kavli Institute of Theoretical Sciences, Chinese Academy of Sciences, Beijing 100049, China*

⁴*Department of Physics, University of Wisconsin-Madison, 1150 University Avenue, Madison, Wisconsin 53706, USA*

⁵*Collaborative Innovation Center of Quantum Matter, Beijing 100871, China*



(Received 13 March 2019; published 25 November 2019)

We study the energy spectrum of Weyl fermions in a topological semimetal in the presence of a central charged impurity. When the strength of the charge exceeds a critical value, an infinite family of quasibound states appear that show characteristic signatures of discrete scale invariance. The invariance is broken by the presence of screening or a finite mass. If these terms are small enough the quasibound states still exist, but there can be perturbations of the shallowest quasibound states. These special quasibound states manifest themselves in the local density of states as well as the relative phase, which can be observed by scanning tunneling microscopy. Such effects that are usually associated with the relativistic quantum electrodynamics of strong fields become observable in topological materials.

DOI: [10.1103/PhysRevB.100.195140](https://doi.org/10.1103/PhysRevB.100.195140)

I. INTRODUCTION

The recent discovery of massless excitations in Weyl and Dirac semimetals [1–6] provides a realization of quantum electrodynamics (QED) in condensed matter systems [7,8]. Like graphene as their two-dimensional analog, Weyl and Dirac semimetals have the conduction and valence bands with the crossing point called a Weyl point [1]. In QED, when the central charge of the nucleus exceeds $Z = 1/\alpha = \hbar c/e^2 \approx 137$, the solutions of the Dirac equation have complex eigenenergies, corresponding to the resonance states related to the supercritical atomic collapse phenomena [9–11]. In these circumstances, the wave functions of these states no longer converge at the origin, necessitating the introduction of a short-range cutoff such as a finite nuclear radius. This then influences the long-range physical properties of the system [9–11]. On the other hand, for a massless Weyl fermion instead of a massive electron, there will be no bound states because of Klein tunneling, and only quasibound states exist when the Coulomb attraction becomes large enough to be in the supercritical regime [12–16]. Because of a low Fermi velocity v_F (generally 2 orders of magnitude smaller than the light speed c in vacuum), the “effective fine-structure constants” $\alpha = e^2/\hbar v_F$ in topological semimetals and graphene are $O(1)$, which gives rise to scale symmetry breaking in these materials away from the perturbative QED paradigm. Previously, theoretical researchers have studied the vacuum polarization and quasibound state properties in graphene with a Coulomb potential [12–17] and the vacuum polarization effect in Dirac semimetals [18]. The vacuum polarization

localized at the impurity position in the subcritical case in graphene is exactly calculated [15]. The supercritical atomic collapse phenomena in graphene and the associated scale anomaly have recently been observed in experiments [19,20].

In a scale-invariant system, quantization effects can spontaneously break the continuous scale invariance down to the discrete scale invariance (DSI). A well-known example of this in quantum physics is the Efimov trimer states [21,22]. In solid-state systems with parabolic dispersion, the scale-invariance condition is hard to meet. However, recent progress in realization of topological semimetals with Coulomb impurities means we now have material systems that fulfill the requirement of scale invariance. Moreover, the small Fermi velocity in topological materials leads to a large effective fine-structure constant, and thus the supercritical collapse condition gives rise to the quasibound states [12–14,16]. The combination of scale invariance and quantization leads to the DSI property of the quasibound states. On the other hand, recent transport experiments in topological semimetal systems have observed anomalous quantum oscillations beyond the quantum limit [23–26]. Further investigations show that these anomalous oscillations obey the approximate DSI property [25,27]. Thus it is of interest to extend the study of DSI to topological semimetals. This needs to include realistic features such as the effects of screening and a finite mass.

In this article, we compute the wave functions and energy spectrum of a Weyl fermion in a three-dimensional (3D) topological semimetal with a charged impurity and find that if the central charge exceeds a certain critical value, there are quasibound states with an energy spectrum obeying the DSI relation $\log |E_n/E_0| \propto n$ for any positive integer n . Every quasibound state manifests itself as a π phase shift in the scattering phase. Unlike the cases discussed in the graphene system,

*haiwen.liu@bnu.edu.cn

we include the screening caused by many-body effects and numerically compute the wave functions as well as the local density of states (LDOS), the peaks of which correspond to the quasibound states. We find that quasibound states still exist in the presence of screening, and the logarithmic spectrum is little perturbed for the deep quasibound states. The main effect of screening is on the shallow bound states and becomes very noticeable when the screening length becomes comparable to the radius of the state. We then proceed to consider the influence of a mass term, and we find that a small mass term has little impact on the DSI-related features of deep quasibound states.

II. MODEL

We consider a Weyl fermion with Fermi velocity v_F in a central field $V(r)$ and neglect the inter-Weyl-nodes coupling. The wave equation reads

$$\hbar v_F \begin{bmatrix} -i\partial_z & -i\partial_x - \partial_y \\ -i\partial_x + \partial_y & i\partial_z \end{bmatrix} \psi = [E - V(r)]\psi. \quad (1)$$

In spherical coordinates r, θ, ϕ , the angular part can be separated out of the Weyl equation, and the solution of Eq. (1) has the form [9,11]

$$\psi_{k\kappa m} = \frac{1}{\sqrt{2r}} (u_{1k\kappa} \chi_{\kappa}^m + iu_{2k\kappa} \chi_{-\kappa}^m), \quad (2)$$

where the momentum $k = -E/\hbar v_F$ is a quantum number proportional to the energy with dimension L^{-1} , and κ, m are dimensionless quantum numbers of angular momentum. The spinor angular functions are as follows:

$$\chi_{\kappa}^m = \begin{cases} \begin{bmatrix} -\sqrt{\frac{j-m+1}{2j+2}} Y_{j+1/2}^{m-1/2} \\ \sqrt{\frac{j+m+1}{2j+2}} Y_{j+1/2}^{m+1/2} \end{bmatrix}, & j = l - \frac{1}{2} \\ \begin{bmatrix} \sqrt{\frac{j+m}{2j}} Y_{j-1/2}^{m-1/2} \\ \sqrt{\frac{j-m}{2j}} Y_{j-1/2}^{m+1/2} \end{bmatrix}, & j = l + \frac{1}{2} \end{cases} \quad \kappa = \begin{cases} j + \frac{1}{2} \\ -(j + \frac{1}{2}) \end{cases}. \quad (3)$$

The $Y_{\ell}^m(\theta, \phi)$ are the usual spherical harmonics. We get the radial equation by substituting Eqs. (2) and (3) into Eq. (1):

$$\frac{d}{dr} \begin{bmatrix} u_{1k\kappa}(r) \\ u_{2k\kappa}(r) \end{bmatrix} = \begin{bmatrix} -\kappa/r & -k - V/\hbar v_F \\ k + V/\hbar v_F & \kappa/r \end{bmatrix} \begin{bmatrix} u_{1k\kappa}(r) \\ u_{2k\kappa}(r) \end{bmatrix}. \quad (4)$$

III. DISCRETE SCALE INVARIANCE UNDER COULOMB POTENTIAL

Let us consider first the case where the potential is a pure Coulomb field generated by an impurity charge Ze . Assume ε is the background effective dielectric constant and introduce new dimensionless variables α, γ, x :

$$V = \hbar v_F \frac{\alpha}{r}, \quad \alpha \equiv \frac{Ze^2}{\varepsilon \hbar v_F}, \quad \gamma = \sqrt{\kappa^2 - \alpha^2}, \quad x = 2ikr. \quad (5)$$

We make the unitary transformation

$$\begin{bmatrix} u_{1k\kappa}(r) \\ u_{2k\kappa}(r) \end{bmatrix} = \frac{1}{\sqrt{2}} \begin{bmatrix} 1 & 1 \\ -i & i \end{bmatrix} \begin{bmatrix} \Phi_{1\kappa}(x) \\ \Phi_{2\kappa}(x) \end{bmatrix}. \quad (6)$$

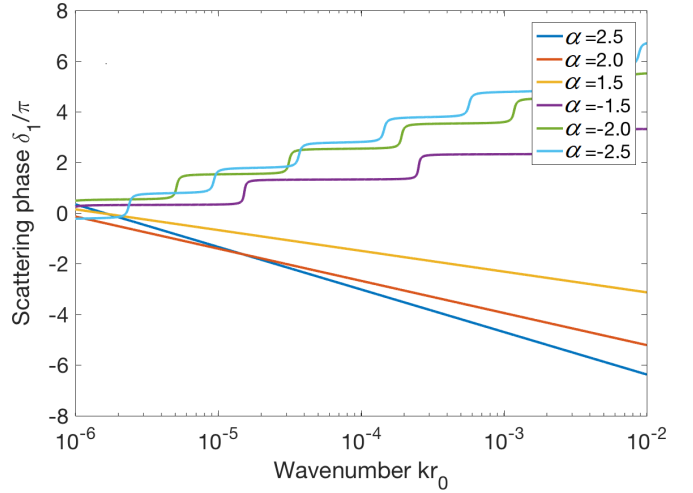


FIG. 1. Relative phase δ_1 in the supercritical case $|\alpha| > 1$ at negative energy $E = -\hbar v_F k < 0$. The kinks correspond to the quasibound states. r_0 is small comparable to the lattice constant.

Equation (4) can then be written in a dimensionless form

$$\frac{d}{dx} \begin{bmatrix} \Phi_{1\kappa}(x) \\ \Phi_{2\kappa}(x) \end{bmatrix} = \begin{bmatrix} \frac{1}{2} + \frac{i\alpha}{x} & -\frac{\kappa}{x} \\ -\frac{\kappa}{x} & -\frac{1}{2} - \frac{i\alpha}{x} \end{bmatrix} \begin{bmatrix} \Phi_{1\kappa}(x) \\ \Phi_{2\kappa}(x) \end{bmatrix}. \quad (7)$$

Equation (7) can be solved analytically and we find

$$\Phi_{1\kappa}(x) = Ax^\gamma e^{-x/2} {}_1F_1(1 + \gamma + i\alpha; 1 + 2\gamma; x) + Bx^{-\gamma} e^{-x/2} {}_1F_1(1 - \gamma + i\alpha; 1 - 2\gamma; x). \quad (8)$$

Here, the ${}_1F_1$ are standard hypergeometric functions, and the $\Phi_{2\kappa}(x)$ can be obtained by Eq. (7) and the explicit form of $\Phi_{1\kappa}(x)$. The solution is simple in the subcritical case $|\alpha| < \kappa$ when γ is real. In this case, we may take $B = 0$, and therefore $\Phi_{1\kappa}(x), \Phi_{2\kappa}(x)$ can be both regular at $r = 0$, corresponding to the outgoing and the incoming waves. The asymptotic form of $\Phi_{1\kappa}/\Phi_{2\kappa}$ leads to a relative phase:

$$\Phi_{1\kappa}/\Phi_{2\kappa} \rightarrow \exp 2i[kr + \alpha \ln 2kr + \delta_\kappa]. \quad (9)$$

The unusual log dependence of the second term results from the long-range $1/r$ field [28], and δ_κ depends only on α, κ . The vacuum polarization effect of the subcritical case, which in two-dimensional graphene has been solved self-consistently [15], manifests itself as a local induced charge in the 3D case as well.

The supercritical case of the partial wave labeled by angular quantum number κ is when $|\alpha| > \kappa$, which determines the critical central charge for the κ wave: $Z_c(\kappa) = \varepsilon \hbar v_F \kappa / e^2$. In this case both terms of $\Phi_{1\kappa}$ in Eq. (8) become singular at the origin because of the imaginary $\gamma = i\gamma', \gamma' \equiv \sqrt{\alpha^2 - \kappa^2}$. We introduce a cutoff distance r_0 comparable with the lattice constant and assume $V(r < r_0)$ is a constant. We comment below on any cutoff dependence of the results. A, B can be solved using this boundary condition. The relative phase can still be written like Eq. (9) but with the scattering phase δ_κ now dependent on α, κ, k . As illustrated in Fig. 1, for a repulsive potential $\alpha > \kappa$, the relative phases have a logarithmic dependence $\delta_\kappa(k) \sim -\gamma' \ln kr_0$.

However, the more important case is the attractive potential $\alpha < -\kappa$, where quasibound states appear as the kinks in $\delta_\kappa(k)$. The energies of the quasibound states exhibit DSI

$$k_n \propto e^{-\frac{\pi n}{\gamma}}, \quad (10)$$

where n is a non-negative integer. The value of the cutoff r_0 and the cutoff procedure generally will affect the (unwritten) coefficient in this equation—the value of k_0 . However, it does not affect the ratio of successive k_n . Similar statements hold for the characteristic wavelengths of the bound states.

Interestingly, these quasibound states can be deduced from a quasiclassical approach using the Wentzel-Kramers-Brillouin (WKB) approximation, which can help us understand DSI [27]. The square of the radial momentum p is

$$p^2 = \left(k + \frac{\alpha}{r}\right)^2 - \frac{\kappa^2}{r^2}. \quad (11)$$

There is a classically forbidden region $r_1 < r < r_2$, $r_{1,2} = (-\alpha \mp \kappa)/k$, where p^2 is negative. The quasibound states are trapped within r_1 and can be found from the Bohr-Sommerfeld quantization condition $\int_{r_0}^{r_1} p dr = \pi \hbar n$, which also leads to Eq. (10). The “radius” of a quasibound state r_1 increases with supercriticality $-\alpha - \kappa$ and decreases with energy k .

IV. EFFECT OF SCREENED COULOMB POTENTIAL

If we consider screening of the potential in topological semimetals, V no longer takes the pure $1/r$ form. The radial equation must be solved numerically. Using the Thomas-Fermi (TF) approximation for the screening [29] in three dimensions, we get the potential

$$V = \hbar v_F \frac{\alpha}{r} e^{-r/\xi}, \quad (12)$$

where the screening length ξ obeys the relation $\xi^{-2} = 4\pi e^2 \frac{dn}{d\mu}$, with $n = \frac{gk_F^3}{6\pi^2}$, $\mu = \hbar v_F k_F$, and g denoting the carrier density, the chemical potential, and the degeneracy, respectively. The TF form used here is appropriate since we expect the screening due to conduction electrons to dominate over the vacuum polarization effects treated in Refs. [12–16]. At the length scales of interest here, the main effect of vacuum polarization will be a downwards renormalization of the charge. In order to solve Eq. (4), we adopt the WKB approximation to get a differential equation for $u_{1k\kappa}$:

$$\frac{d^2 u_{1k\kappa}}{dr^2} + \left[\left(k + \frac{\alpha}{r} e^{-\frac{r}{\xi}}\right)^2 - \frac{\kappa^2}{r^2} \right] u_{1k\kappa} = 0. \quad (13)$$

The exact differential equation includes other terms of $O(r^{-1})$ which are neglected in the small r limit. In this potential, the square of radial momentum p^2 is the expression in square brackets. There are again two turning points r_1, r_2 and a classically forbidden region $p^2 < 0$ in between, just as in the pure Coulomb potential case. The WKB approximation gives the solution of $u_{1k\kappa}$ in the three different regions, depending on the sign of p^2 : (i) $r_0 < r < r_1$, (ii) $r_1 < r < r_2$, and

(iii) $r > r_2$:

$$u_{1k\kappa}(r) = \begin{cases} \frac{1}{\sqrt{p}} (A_1 e^{i \int_{r_1}^r p dr'} + A_2 e^{-i \int_{r_1}^r p dr'}) & \text{(i)} \\ \frac{1}{\sqrt{\tilde{p}}} (B_1 e^{-\int_{r_2}^r \tilde{p} dr'} + B_2 e^{\int_{r_2}^r \tilde{p} dr'}) & \text{(ii)} \\ \frac{1}{\sqrt{p}} (C_1 e^{i \int_{r_2}^r p dr'} + C_2 e^{-i \int_{r_2}^r p dr'}) & \text{(iii)}, \end{cases} \quad (14)$$

where $\tilde{p}^2 = -p^2$. Near r_1 or r_2 , we use the Airy function of Eq. (13) to get connection formulas that are then solved for A_1, A_2, \dots, C_2 . This allows us to compute the LDOS of the κ partial wave. We find there are still quasibound states in the screened potential, but the DSI-related log periodicity of the energy levels is affected by the screening (see Fig. 2). Specifically, the logarithmic level spacing $\ln(k_n/k_{n-1})$ increases as the momentum scale k_n decreases. If we increase screening (decrease ξ), the level spacing becomes larger and fewer levels are visible in the LDOS, as shown in Figs. 2(a) and 2(b). This breaking of DSI can be viewed as a consequence of the introduction of the length parameter ξ in V . When $\xi \rightarrow \infty$, DSI is restored.

We can also compute the relative phase of the κ partial wave. The kinks when it is plotted as a function of energy correspond to the quasibound energy levels (see Fig. 3). Unlike the “upward” kinks in the pure Coulomb case, the kinks here are “downwards,” because $\alpha \ln 2kr$ makes a negative contribution to the phase but does not affect the position of the kinks.

V. EFFECT OF MASS TERM

We now consider the influence of a mass M . Since this introduces a new length scale it will also break the DSI down to approximate DSI for certain quasibound states. The system is still spherically symmetrical, and after expanding in spinor spherical harmonic functions such as above one can obtain the radial equation with mass term [9,10]:

$$\frac{d^2 u_{1k\kappa}}{dr^2} + \left[\left(k + \frac{\alpha}{r}\right)^2 - \frac{\kappa^2}{r^2} - m_0^2 \right] u_{1k\kappa} = 0, \quad (15)$$

where $m_0 = Mv_F/\hbar$ is the mass parameter with dimension L^{-1} . In this case the two turning points can be expressed explicitly as

$$r_{1,2} = \frac{-\alpha \mp \sqrt{\kappa^2 + \gamma'^2 m_0^2/k^2}}{k(1 - m_0^2/k^2)}. \quad (16)$$

For small mass $m_0/k \ll 1$, both points deviate slightly from the massless result $r_{1,2} = (-\alpha \mp \kappa)/k + O(m_0^2/k^2)$. Thus the quasibound states continue to exist, provided the second term in the following equation is much smaller than the first term:

$$k_n \approx \frac{-\alpha - \kappa}{r_0} e^{-\frac{\pi n}{\gamma'}} - \frac{m_0^2 r_0}{2\kappa} e^{\frac{\pi n}{\gamma'}}. \quad (17)$$

Given $-\alpha > \kappa > 0$, k_n is an monotonically decreasing function of n . If n is not too large, i.e., k_n is large and positive, then energy levels can still be expressed by Eq. (10), preserving DSI in the large energy region. In the screened case, the problem is treated numerically and shown in Fig. 4. In this scenario, only the smallest kinks are affected when m_0 approaches them. In the energy region $k \gg m_0$, the mass term

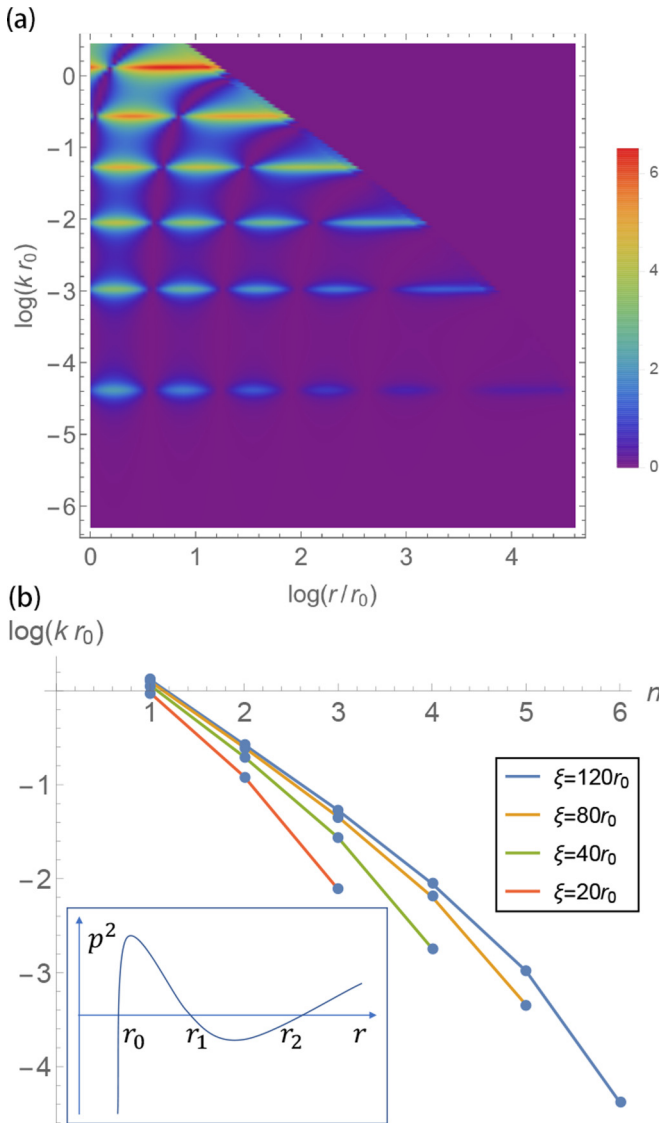


FIG. 2. (a) LDOS $\rho(k, r)$ between r_0 and r_1 of the $\kappa = 1$ partial wave at screening $\xi = 120r_0$ and central charge $\alpha = -5$. The peaks correspond to the quasibound states. The logarithmic level spacing $\ln(k_n/k_{n-1})$ becomes larger with smaller energy scale k_n . (b) Energy levels of quasibound states for different ξ with $\alpha = -5$. If we increase screening (decrease ξ), the level spacing becomes larger, making fewer levels visible in the LDOS. Inset: A schematic diagram of p^2 ; the quasibound states are largely located in the classically permitted region $r_0 < r < r_1$.

has virtually no influence on the DSI or the location of the kinks. The supercritical charge for system with the finite mass has been previously solved in high-energy physics [9,11], and the related details are reviewed in Ref. [10]. Our main purpose here is to see the influence of a small mass term on the supercritical DSI feature and its manifestation in solid systems, which are not discussed in those pioneering works.

VI. RELATED MATERIALS

The effects proposed in this paper that result from the existence of DSI and quasibound states should be realizable in

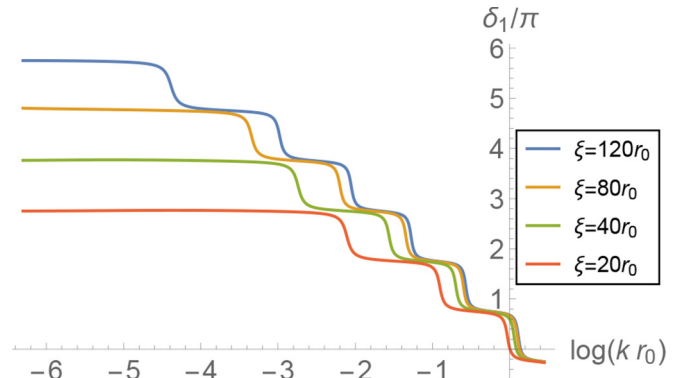


FIG. 3. Scattering phase shift of the $\kappa = 1$ partial wave at different screening lengths ξ with $\alpha = -5$. The kinks correspond to the quasibound energy levels, in agreement with Fig. 2(b).

real topological materials. The main experimental signature to date of DSI is the presence of anomalous log-periodic quantum oscillations when the applied magnetic field is beyond the quantum limit. The lattice constant r_0 of the topological semimetals in which these phenomena is observed is in the range of a few angstroms [4,5,30], while the carrier density is in the range of $10^{15} - 10^{16} \text{ cm}^{-3}$ in these materials [23–26]. Based on the Thomas-Fermi screening relation $\xi^{-2} = \frac{2ge^2k_F^2}{\pi\hbar v_F}$ with degeneracy $g = 4$ (characteristic of most of these materials) [25,26], ξ is approximately $50 \sim 10^2 r_0$. In this case there are generally several energy levels that show DSI, as seen in Fig. 2(a). For example, if $|\alpha| = 5$, then the radii R_n of the states satisfy $R_{n+1}/R_n = \exp(\pi/\sqrt{\alpha^2 - 1}) = 1.90$, and the number of quasibound states with DSI is in the range of 6–7. It should be noted that the value of the short-range cutoff r_0 does not influence DSI: R_{n+1}/R_n is independent of r_0 . However, r_0 does give the energy of the deepest quasibound states and thus, together with the screening length, determines the numbers of quasibound states whose energies form a geometric series.

In the real materials at issue here, any mass gaps are too small to have shown up unambiguously in experiments so far. Nevertheless, there remains the possibility of a very small gap in some cases [23]. In this circumstance the Hamiltonian becomes a Dirac one with a very small rest mass M , as we have seen above, and Eqs. (4) and (13) must be modified.

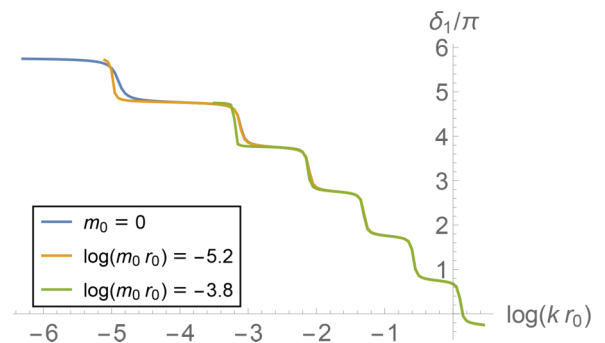


FIG. 4. Scattering phase shift of the $\kappa = 1$ partial wave for different mass parameters m_0 with $\xi = 100 r_0$, and $\alpha = -5$. The kink k_n changes if it is less than or near m_0 . m_0 has virtually no influence on the kinks in the region $k \gg m_0$.

However, the energy levels and DSI effects are not changed provided the energy is much larger than the rest mass, $k \gg m_0 = Mv_F/\hbar$. The energy region probed in the quantum oscillation experiments is $|E| = \hbar v_F k > 10$ meV, so if $Mv_F^2 \approx 1 - 10$ meV, we still expect to see the effects of DSI.

VII. CONCLUSION

We demonstrate the emergence of quasibound states in three-dimensional topological semimetal systems with supercritical charged impurities. In a pure Coulomb field, these states have discrete scale invariance that shows up as energy levels equally spaced on a logarithmic scale. These states with DSI still exist after considering the static screening effect from a small Fermi surface, but the discrete scale invariance is affected, with stretched logarithmic spacing between the shallow quasibound states. These quasibound states are robust against a small finite mass gap at the Weyl point. Recent

transport experiments have observed the anomalous quantum oscillations beyond the quantum limit [23,24] and the $\ln B$ periodic magnetoresistance oscillation in topological materials [25,26], and meanwhile, previous theoretical investigation is devoted to analyzing these exotic transport phenomena [27]. In comparison, the present work concentrates on the local density of states, which can be examined by the scanning tunneling microscope technique.

ACKNOWLEDGMENTS

We thank Ziqiang Wang and Qingfeng Sun for valuable discussions. This work was financially supported by the National Basic Research Program of China (Grants No. 2017YFA0303301 and No. 2015CB921102), the National Natural Science Foundation of China (Grants No. 11674028, No. 11534001, and No. 11504008).

-
- [1] X. Wan, A. M. Turner, A. Vishwanath, and S. Y. Savrasov, Topological semimetal and Fermi-arc surface states in the electronic structure of pyrochlore iridates, *Phys. Rev. B* **83**, 205101 (2011).
- [2] O. Vafeek and A. Vishwanath, Dirac fermions in solids: From high-Tc cuprates and graphene to topological insulators and Weyl semimetals, *Annu. Rev. Condens. Matter Phys.* **5**, 83 (2014).
- [3] B. Q. Lv, H. M. Weng, B. B. Fu, X. P. Wang, H. Miao, J. Ma, P. Richard, X. C. Huang, L. X. Zhao, G. F. Chen, Z. Fang, X. Dai, T. Qian, and H. Ding, Experimental Discovery of Weyl Semimetal TaAs, *Phys. Rev. X* **5**, 031013 (2015).
- [4] S.-Y. Xu, I. Belopolski, N. Alidoust, M. Neupane, C. Zhang, R. Sankar, S.-M. Huang, C.-C. Lee, G. Chang, B. Wang, G. Bian, H. Zheng, D. S. Sanchez, F. Chou, H. Lin, S. Jia, and M. Z. Hasan, Discovery of a Weyl fermion semimetal and topological Fermi arcs, *Science* **349**, 613 (2015).
- [5] X. Huang, L. Zhao, Y. Long, P. Wang, D. Chen, Z. Yang, H. Liang, M. Xue, H. Weng, Z. Fang, X. Dai, and G. Chen, Observation of the Chiral-Anomaly-Induced Negative Magnetoresistance in 3D Weyl Semimetal TaAs, *Phys. Rev. X* **5**, 031023 (2015).
- [6] C. Zhang, S.-Y. Xu, I. Belopolski, Z. Yuan, Z. Lin, B. Tong, N. Alidoust, C.-C. Lee, S.-M. Huang, T.-R. Chang, H.-T. Jeng, H. Lin, M. Neupane, D. S. Sanchez, H. Zheng, G. Bian, J. Wang, C. Zhang, H.-Z. Lu, S.-Q. Shen, T. Neupert, M. Z. Hasan, and S. Jia, Signatures of the Adler-Bell-Jackiw chiral anomaly in a Weyl fermion semimetal, *Nat. Commun.* **7**, 10735 (2016).
- [7] A. G. Grushin, Consequences of a condensed matter realization of Lorentz-violating QED in Weyl semi-metals, *Phys. Rev. D* **86**, 045001 (2012).
- [8] Y. Chen, S. Wu, and A. A. Burkov, Axion response in Weyl semimetals, *Phys. Rev. B* **88**, 125105 (2013).
- [9] Y. B. Zeldovich and V. S. Popov, Electronic structure of superheavy atoms, *Usp. Fiz. Nauk* **105**, 403 (1971) [*Sov. Phys. Usp.* **14**, 673 (1972)].
- [10] V. S. Popov, Critical charge in quantum electrodynamics, *Phys. At. Nucl.* **64**, 367 (2001).
- [11] W. Greiner, B. Müller, and J. Rafelski, *Quantum Electrodynamics of Strong Fields*, 1st ed. (Springer, Berlin, Heidelberg, 1985).
- [12] A. V. Shytov, M. I. Katsnelson, and L. S. Levitov, Vacuum Polarization and Screening of Supercritical Impurities in Graphene, *Phys. Rev. Lett.* **99**, 236801 (2007).
- [13] A. V. Shytov, M. I. Katsnelson, and L. S. Levitov, Atomic Collapse and Quasi—Rydberg States in Graphene, *Phys. Rev. Lett.* **99**, 246802 (2007).
- [14] V. M. Pereira, J. Nilsson, and A. H. Castro Neto, Coulomb Impurity Problem in Graphene, *Phys. Rev. Lett.* **99**, 166802 (2007).
- [15] I. S. Terekhov, A. I. Milstein, V. N. Kotov, and O. P. Sushkov, Screening of Coulomb Impurities in Graphene, *Phys. Rev. Lett.* **100**, 076803 (2008).
- [16] Y. Nishida, Vacuum polarization of graphene with a supercritical Coulomb impurity: Low-energy universality and discrete scale invariance, *Phys. Rev. B* **90**, 165414 (2014).
- [17] Y. Nishida, Renormalization group analysis of graphene with a supercritical Coulomb impurity, *Phys. Rev. B* **94**, 085430 (2016).
- [18] P. Zhang and H. Zhai, Efimov effect in the Dirac semi-metals, *Front. Phys.* **13**, 137204 (2018).
- [19] Y. Wang, D. Wong, A. V. Shytov, V. W. Brar, S. Choi, Q. Wu, H.-Z. Tsai, W. Regan, A. Zettl, R. K. Kawakami, S. G. Louie, L. S. Levitov, and M. F. Crommie, Observing atomic collapse resonances in artificial nuclei on graphene, *Science* **340**, 734 (2013).
- [20] O. Ovdad, J. Mao, Y. Jiang, E. Y. Andrei, and E. Akkermans, Observing a scale anomaly and a universal quantum phase transition in graphene, *Nat. Commun.* **8**, 507 (2017).
- [21] V. Efimov, Energy levels arising from resonant two-body forces in a three-body system, *Phys. Lett. B* **33**, 563 (1970).
- [22] E. Braaten and H. W. Hammer, Universality in few-body systems with large scattering length, *Phys. Rep.* **428**, 259 (2006).
- [23] K. Behnia, L. Balicas, and Y. Kopelevich, Signatures of electron fractionalization in ultraquantum bismuth, *Science* **317**, 1729 (2007).

- [24] C. Zhang, B. Tong, Z. Yuan, Z. Lin, J. Wang, J. Zhang, C.-Y. Xi, Z. Wang, S. Jia, and C. Zhang, Signature of chiral fermion instability in the Weyl semimetal TaAs above the quantum limit, *Phys. Rev. B* **94**, 205120 (2016).
- [25] H. Wang, H. Liu, Y. Li, Y. Liu, J. Wang, J. Liu, J. Dai, Y. Wang, L. Li, J. Yan, D. Mandrus, X. C. Xie, and J. Wang, Discovery of log-periodic oscillations in ultraquantum topological materials, *Sci. Adv.* **4**, eaau5096 (2018).
- [26] H. Wang, Y. Liu, Y. Liu, C. Xi, J. Wang, J. Liu, Y. Wang, L. Li, S. P. Lau, M. Tian, J. Yan, D. Mandrus, J.-Y. Dai, H. Liu, X. C. Xie, and J. Wang, Log-periodic quantum magneto-oscillations and discrete scale invariance in topological material HfTe₅, *Nat. Sci. Rev.* nwz110 (2019).
- [27] H. Liu, H. Jiang, Z. Wang, R. Joynt, and X. C. Xie, Discrete scale invariance in topological semimetals, [arXiv:1807.02459](https://arxiv.org/abs/1807.02459).
- [28] L. D. Landau and E. M. Lifshitz, *Quantum Mechanics*, 3rd ed. (Pergamon, London, 1977), Chap. XVII, p. 135.
- [29] M. I. Katsnelson, Nonlinear screening of charge impurities in graphene, *Phys. Rev. B* **74**, 201401(R) (2006).
- [30] C.-C. Lee, S.-Y. Xu, S.-M. Huang, D. S. Sanchez, I. Belopolski, G. Chang, G. Bian, N. Alidoust, H. Zheng, M. Neupane, B. Wang, A. Bansil, M. Z. Hasan, and H. Lin, Fermi surface interconnectivity and topology in Weyl fermion semimetals TaAs, TaP, NbAs, and NbP, *Phys. Rev. B* **92**, 235104 (2015).